

Profile data base for cloudy and rainy atmospheres

Jean-François Mahfouf

25 June 2013

1. Introduction

This document describes the methodology proposed in order to evaluate the information content from a future microwave radiometer ranging between 1 and 1000 GHz in cloudy and rainy atmospheres. The methodology is somewhat different from the one used for clear sky atmospheres for a number of reasons described afterwards.

The information content is based on the estimation theory that is build on the knowledge of the errors from an a-priori information provided by ECMWF short range forecasts (background error covariance matrix \mathbf{B}), the errors on the instrumental side (observation error covariance matrix \mathbf{R}), and the Jacobian matrix (\mathbf{H}) that provides the sensitivity of simulated brightness temperatures to atmospheric model profiles (given by the ARTS radiative transfer model). The combination of these three ingredients allows to compute the *Degrees of Freedom for Signal* as $DFS = Tr(\mathbf{I} - \mathbf{A}\mathbf{B}^{-1})$ and the *Entropy Reduction* as $ER = 0.5(\log_2(\mathbf{B}) - \log_2(\mathbf{A}))$ where \mathbf{A} is the covariance matrix of analysis errors : $\mathbf{A} = (\mathbf{B}^{-1} + \mathbf{H}^T\mathbf{R}^{-1}\mathbf{H})^{-1}$. These computations have to be done for a number of representative profiles. The information content is examined *separately*¹ for each atmospheric variables : temperature (T), specific humidity (q), cloud liquid water content (w_l), cloud ice water content (w_i), rain water content (w_r), snow water content (w_s). For each of these variables and for each profile a specific matrix of background errors has to be specified. This is rather straightforward for T and q (see Hulm and Kral (2012)) since these quantities are necessary in most variational data assimilation systems, and the dependency with each individual profile is only significant for the variance of q . On the other hand, the estimation of a \mathbf{B} matrix for variables describing the condensed phases of water is more difficult since the errors are highly dependent upon the profile of interest and are generally not produced in global variational assimilation systems such as at ECMWF (since these variables are not explicitly initialised). Studies are currently undertaken for the estimation of such matrices but small scale models with explicit convection (Montmerle and Berre, 2010; Michel et al., 2011). We describe hereafter a strategy chosen in a previous study at ECMWF (Di Michele and Bauer, 2006) and considered for the current project.

2. The base of profiles

The atmospheric profiles are taken from short range forecasts from the ECMWF model (CY32R3) that has been run with a T799 spectral truncation (25 km) and 91 vertical levels from July 2006 to

1. This choice comes from the fact that a global information content study would heavily rely on correlations between variables in the \mathbf{B} matrix and on the relative sizes of the variances that have non negligible level of uncertainty. It also explains why the cross-correlation matrices between the hydrometeor variables are not displayed in the next section.

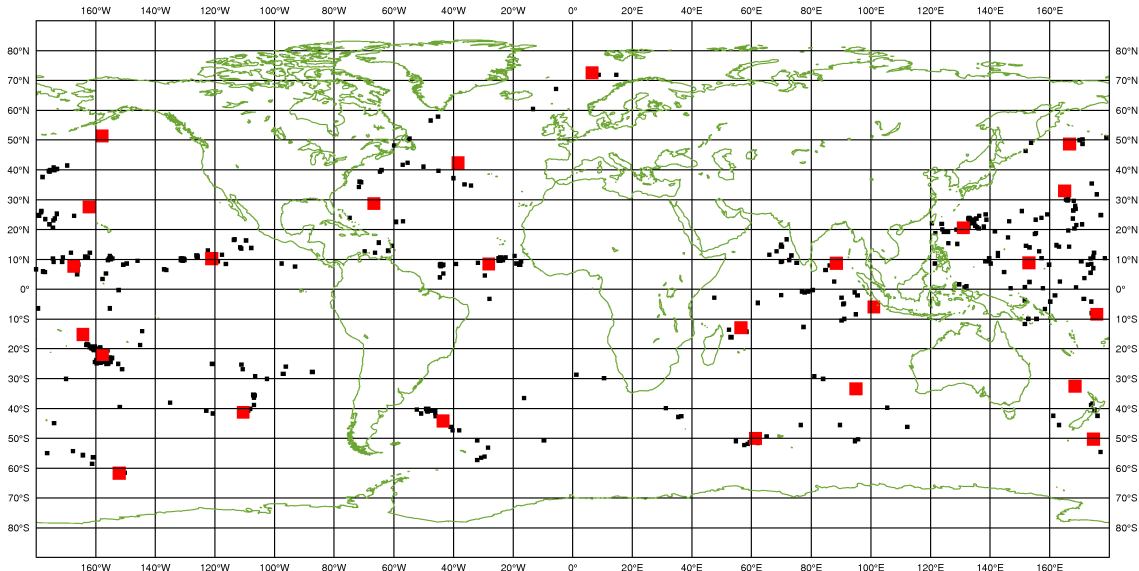


FIGURE 1 – Set of 613 profiles over oceans taken from an ECMWF 48h forecast starting on 10th July 2006 (black squares). The red squares indicate the chosen locations for a first selection of 25 profiles.

June 2007. Forecasts are relative to 42, 48, 54 and 60 hours of day 1, 10 and 20 of every month. The data base has been kindly provided by Sabatino Di Michele (ECMWF). This base is rather similar to the one from Chevallier et al. (2006). However, it contains additional information necessary to compute background error statistics for hydrometeor contents (Table 1). Indeed, since hydrometeors are not part of the control variable in the ECMWF 4D-Var, the corresponding background error statistics are not available. Therefore the methodology proposed by Hulm et Kral (2012) for temperature and specific humidity cannot be use for these quantities.

3. Background error covariance matrices

Background error covariance matrices for hydrometeors can be computed from the background error covariance matrices for temperature T and specific humidity q using linearized physical parameterisation schemes.

Indeed, moist physical parameterization schemes for large scale condensation and deep and shallow convections can be represented by an operator \mathcal{H} that generates profiles of hydrometeor contents and cloud cover given input profiles of T and q . The output profiles are : the fractional cloud cover cc , the cloud liquid water content w_l , the cloud ice water content w_i , the liquid precipitation rate w_r , and the solid precipitation rate w_s .

$$(cc, w_l, w_i, w_r, w_s) = \mathcal{H}(T, q) \quad (1)$$

Using such operator, it is possible to express the relation between the covariance matrices of background errors for $x = (T, q)$ and for $y = (cc, w_l, w_i, w_r, w_s)$:

$$\mathbf{B}_y = \mathbf{H}\mathbf{B}_x\mathbf{H}^T \quad (2)$$

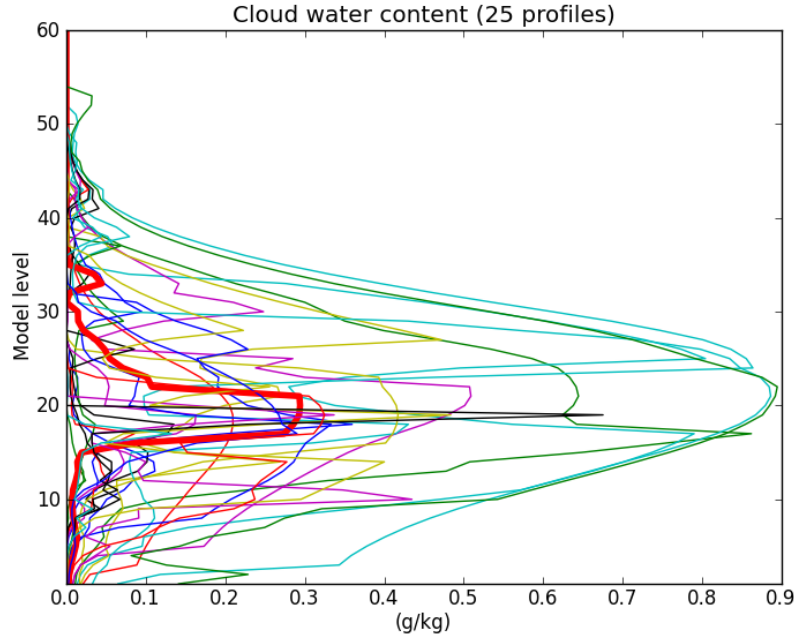


FIGURE 2 – Vertical profiles of cloud water contents (sum of liquid and solid) at the 25 selected locations shown in Figure 1. The profile in red bold corresponds to the selected location to illustrate the background covariances matrices.

The above formula requires the tangent-linear \mathbf{H} and the adjoint versions \mathbf{H}^T of the moist physical processes. Such linearized physical processes have been developed at ECMWF by Lopez and Moreau (2005) for the moist convection and by Tompkins and Janiskova (2004) for stratiform precipitation and cloud cover. They are used in the operational ECMWF four dimensional variational assimilation system and allow the assimilation of cloudy microwave radiances and surface precipitation rates. The physical processes are simplified with respect to the one used in the non-linear model but produce rather similar results while making the tangent-linear approximation valid for finite size perturbations. In addition to temperature and humidity profiles, these physical parameterizations also need additional information regarding the surface and large-scale forcings (turbulent fluxes, time tendencies) in order to produce a realistic response (see Table 1). It explains why the availability of \mathbf{H} and \mathbf{H}^T with the Chevallier et al. (2006) data base is not sufficient to get covariance matrices of background errors for hydrometeors.

4. Preliminary selection of profiles

In order to examine the information content for cloudy and rainy profiles we have taken a set of profiles from the 48h forecast starting at 12 UTC on the 10/07/2006 over ocean surfaces (for simpler description of the surface emissivity). For this forecast range, 613 profiles are available, and we have selected 25 of them that are sampled over contrasted regions (Figure 1). Indeed, the computation of the Jacobians with the ARTS model is rather time consuming since it is done in finite differences. The variability of the 25 profiles is shown in Figure 2 for the total cloud water content expressed in g/kg. For illustration purposes, we have selected the first profile located in the Atlantic Ocean

Variable	Units	rank
Temperature	K	1-91
Specific humidity	kg/kg	92-182
Temperature tendency	K/s	183-273
Specific humidity tendency	(kg/kg/s)	274-364
Surface pressure (log)	Pa	365
Surface sensible heat flux	W/m ²	366
Surface latent heat flux	W/m ²	367
Surface stress (U)	kg/m ² /s	368
Surface stress (V)	kg/m ² /s	369
Cloud cover	(0-1)	370-460
Cloud liquid water	kg/kg	461-551
Cloud ice water	kg/kg	552-642
Rain flux	kg/m ² /s	643-733
Snow flux	kg/m ² /s	734-824
Geopotential	m ² /s ²	825
Land-sea mask	(0-1)	826
Latitude	deg	827
Longitude	deg	828
Year		829
Month		830
Day		831
Step		832
Grid point		833
Index		834

TABLE 1 – Variables provided in the extended ECMWF database of profiles (T799L91 model version)

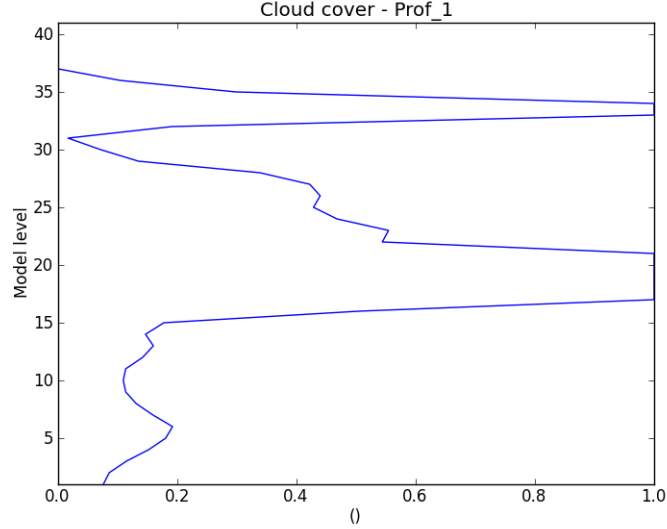


FIGURE 3 – Vertical profile of cloud fraction produced for the profile 1 of the ECMWF data base for hydrometeors (10/07/2006)

(72.517 N, 6.48 E) for which the condensed variables in Figures 3 and 4 (also highlighted in Figure 2).

5. An example of background error covariance matrices for hydrometeors

The matrices are displayed in terms of correlations and standard deviations separately. The correlation matrices for the temperature and specific humidity profiles are shown in Figure 5, with the corresponding profiles of background errors in Figure 6. In agreement with the known structure of these errors, the correlations are rather sharp on the vertical with only positive values for q and slight negative values for T for adjacent levels in the free atmosphere. Correlations are more important in the boundary layer (between levels 1 and 10) due to the vertical mixing induced by turbulence. Regarding the standard deviations, for T a value around one is found in the troposphere with a significant increase in the stratosphere up to 6 K ; for q the rapid decrease with altitude is consistent with the corresponding decrease of specific humidity (not shown).

The application of the linearized physics operators \mathbf{H} and \mathbf{H}^T to the above \mathbf{B}_x matrix leads to the correlation matrices \mathbf{B}_x (Equation 2) shown in Figures 7 and 8. For liquid precipitation (w_r) there is a correlation of one between levels 1 and 10 corresponding to the region where only liquid precipitation is present. In the mixed phase, the correlation also very high but restricted to this specific area. High correlations are also noticed between levels where solid precipitation (w_s) is falling. The reduced correlations noticed between levels 22 and 30 correspond to a region with lower cloud cover. Similarly, the high localised correlations noticed around level 32 are associated with the thin cloud layer noticed in the vertical profile (Figure 3). For non-precipitating hydrometeors, vertical correlations are more localised except in the lowest levels and in the layer around level 25 where the cloud fraction is equal to one. When examining the standard deviation of background errors (Figure 8) , the vertical structure of the errors appears consistent with the profiles of the corresponding variables. However

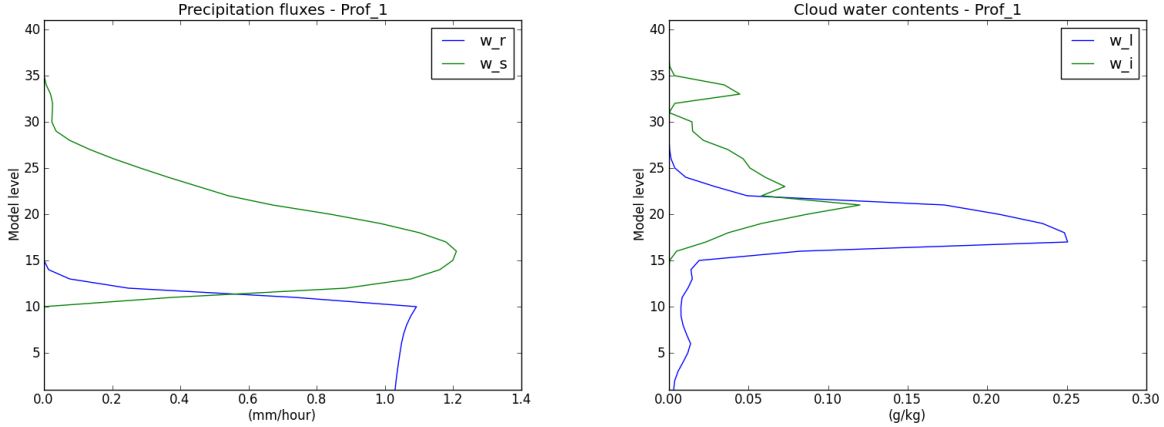


FIGURE 4 – Vertical profiles of liquid (w_l) and solid (w_s) precipitation fluxes (mm/h) (left panel) and cloud liquid (w_l) and ice (w_i) water contents (g/kg) (right panel) produced for the profile 1 of the ECMWF data base for hydrometeors (10/07/2006)

the errors for liquid precipitation are much smaller than the ones for solid precipitation. Similarly for liquid and ice water contents, the errors are significantly smaller for liquid water than for ice water, except at level 15 where a large error up to 0.27 g/cm³ is computed. This level is associated with a strong increase of the liquid water with height together with an increase in cloud cover (basically the signature of cloud base). It is likely that such sharp gradients are not adequately described by the linearized physics.

6. Conclusions

We have presented a data base of ECMWF profiles suitable for examining the information content of satellite radiances to hydrometeors. It complements the Chevallier et al. (2006) data base that does not contain enough information in order to project the background error covariance matrices for T and q on the various variables describing the condensed variables. This has been using the moist linearized physical package from ECMWF (Tompkins and Janiskova, 2004; Lopez and Moreau, 2005). Such methodology initially proposed by Di Michele and Bauer (2006) allows to provide background error statistics for hydrometeors that are consistent with the actual profiles, which is compulsory given the large natural variability of such quantities. A set of 25 profiles have been selected for the computation of the Jacobians of the ARTS model. If necessary other profiles could be considered since the data base contains thousands of profiles with the corresponding \mathbf{B} matrices.

Acknowledgements

The author is grateful to Sabatino Di Michele (ECMWF) for providing to the project the material described in this report.

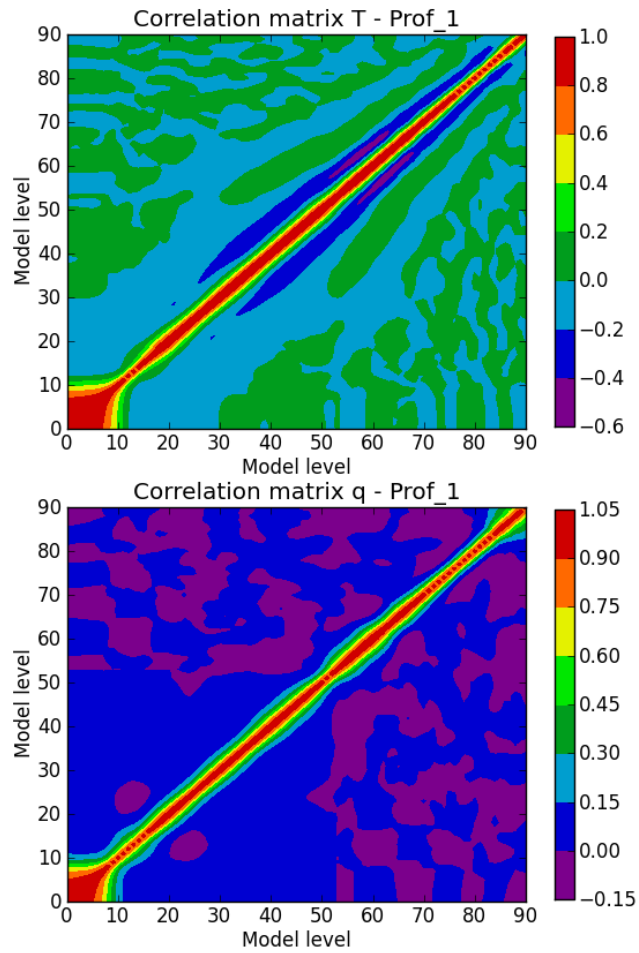


FIGURE 5 – Background error correlation matrices for T and q associated with Profile 1

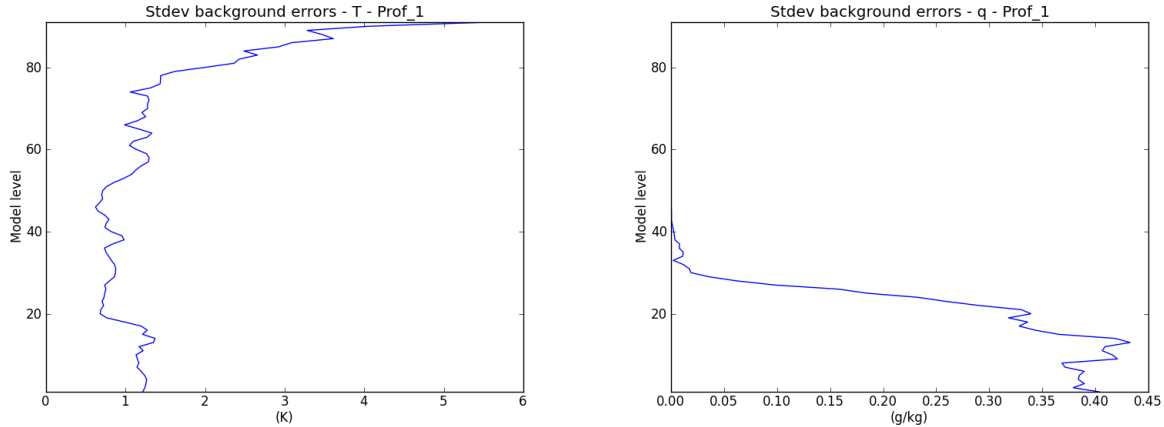


FIGURE 6 – Standard deviation of background errors for T (in K) and q (in g/kg) associated with Profile 1

References

- F. Chevallier, S. Di Michele, and A. P. McNally, 2006 : Diverse profile datasets from the ECMWF 91-level short-range forecasts. *NWP SAF technical report N°10*, 14pp
- Y. Michel, T. Auligné, and T. Montmerle, 2011 : Heterogeneous convective-scale background error covariances with the inclusion of hydrometeor variables. *Monthly Weather Review*, **139**, D20104, 2994-3015
- Di Michele, S. and P. Bauer, 2006 : Passive microwave radiometer channel selection based on cloud and precipitation information content estimation. *Quart. J. Roy. Meteor. Soc.*, **132**, 1299-1324
- E. Hulm, and T. Kral, 2012 : Flow-dependent, geographically varying background error covariances for 1D-VAR applications in MTG-IRS L2 processing *ECMWF Technical Memorandum N°680*, 15 pp.
- T. Montmerle, and L. Berre, 2010 : Diagnosis and formulation of heterogeneous background error covariances at mesoscale. *Quart. J. Roy. Meteor. Soc.*, **136**, 1408-1420
- P. Lopez and E. Moreau, 2005 : A convective scheme for data assimilation : Description and initial tests. *Quart. J. Roy. Meteor. Soc.*, **131**, 409-436
- A.M. Tompkins, and M. Janiskova, 2004 : A cloud scheme for data assimilation : Description and initial tests. *Quart. J. Roy. Meteor. Soc.*, **130**, 2495–2518.

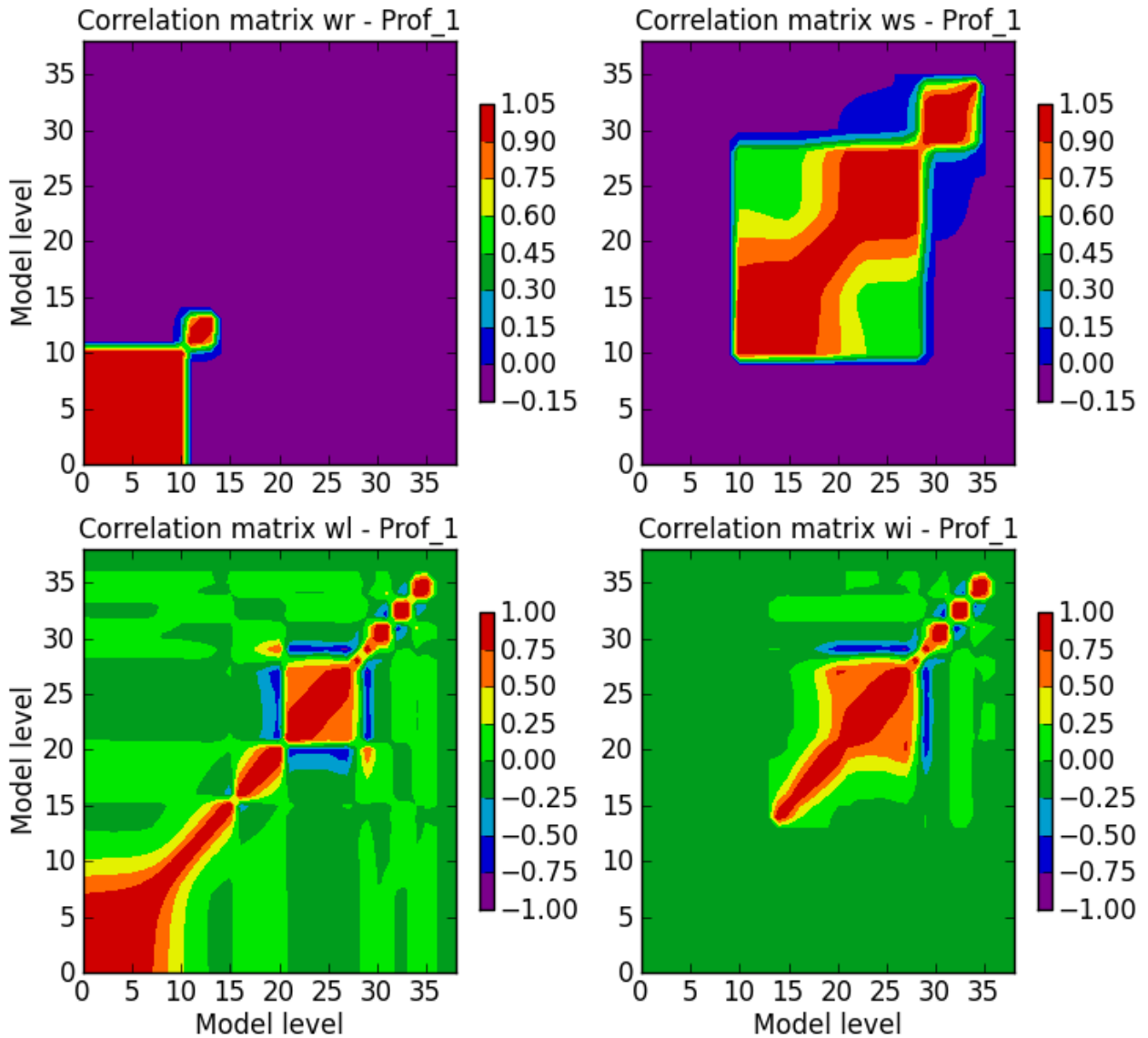


FIGURE 7 – Vertical correlations of hydrometeors computed from the ECMWF linearized physics with Profile 1 : liquid rain (upper left), solid rain (upper right), liquid cloud (lower left), and solid cloud (lower right)

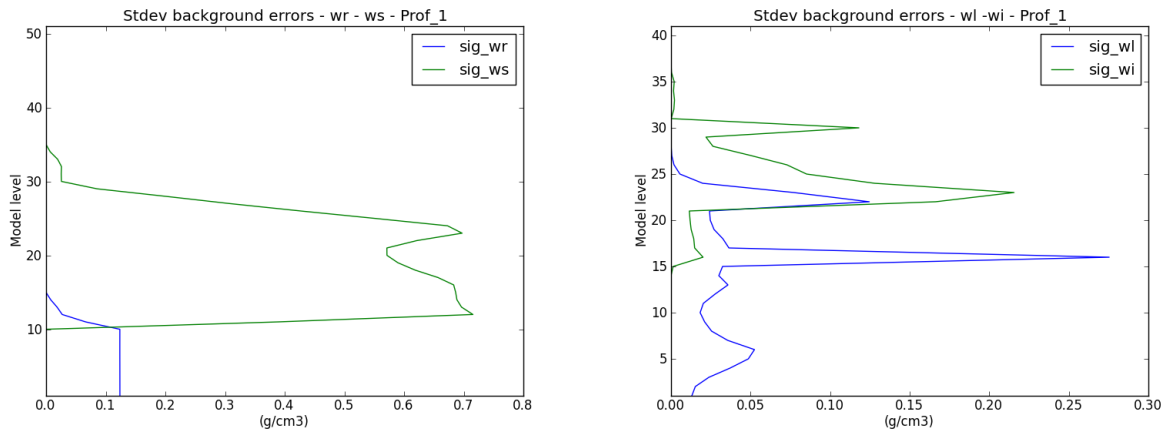


FIGURE 8 – Standard deviation of background errors computed from the ECMWF linearized physics with Profile 1 : liquid and solid rain water contents (left) and liquid and cloud water contents (right). A conversion has been made between precipitation rates RR and precipitating hydrometeor contents w_r using a formula available in the radiative transfer code RTTOV.